



Supplement of

Seasonal reconstructions coupling ice core data and an isotope-enabled climate model – methodological implications of seasonality, climate modes and selection of proxy data

Jesper Sjolte et al.

Correspondence to: Jesper Sjolte (jesper.sjolte@geol.lu.se)

The copyright of individual parts of the supplement might differ from the CC BY 4.0 License.

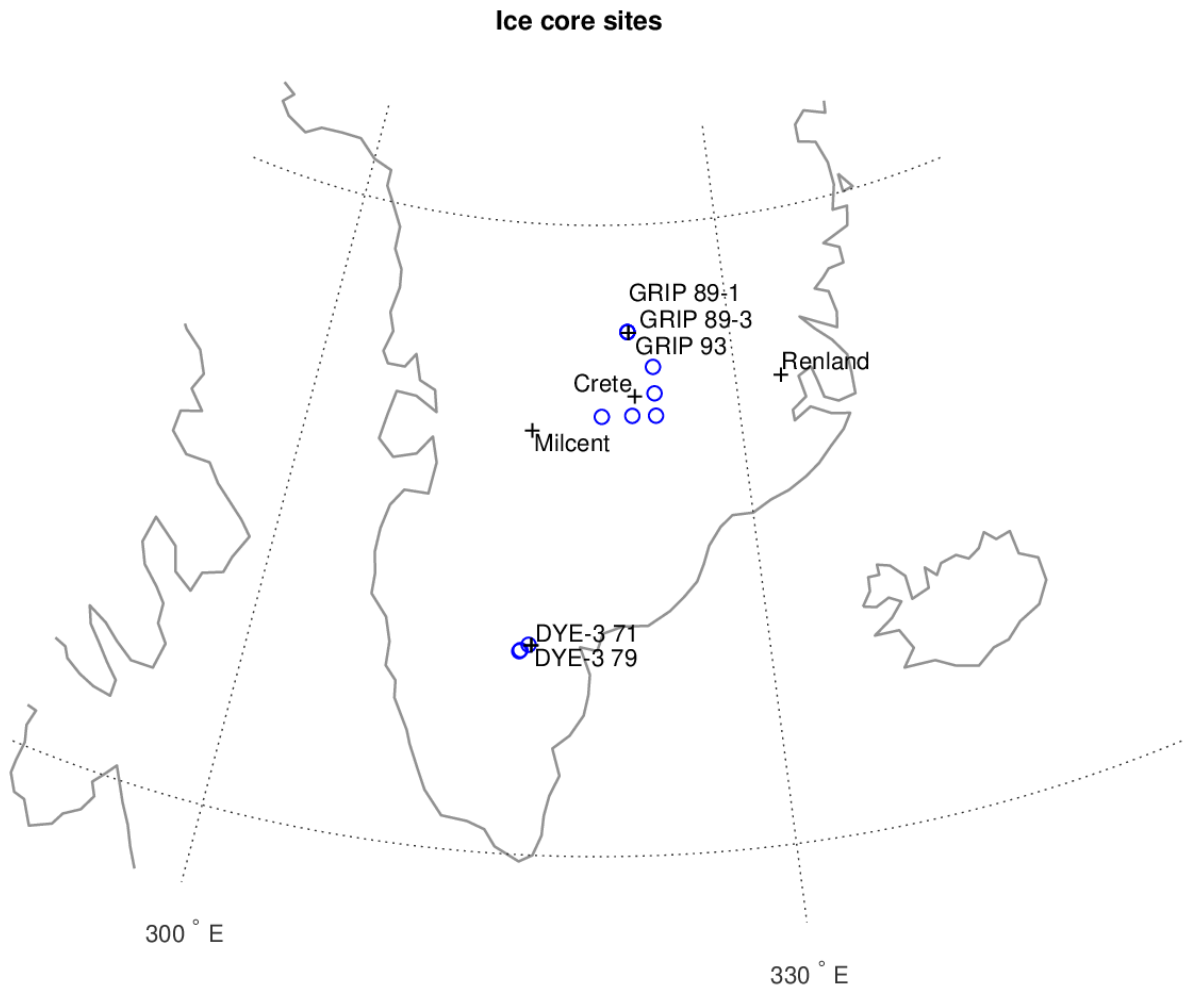


Figure S1: Locations of sites for the 8 ice cores for the period 1241-1970 (black) and additional ice cores covering 1778-1970 (blue) bringing the total number up to 19 ice cores for the shorter time span. The 19 cores include a total of 5 cores from DYE-3 and 6 cores from GRIP, as well as Site A, B, D, E and G located close to Crete.

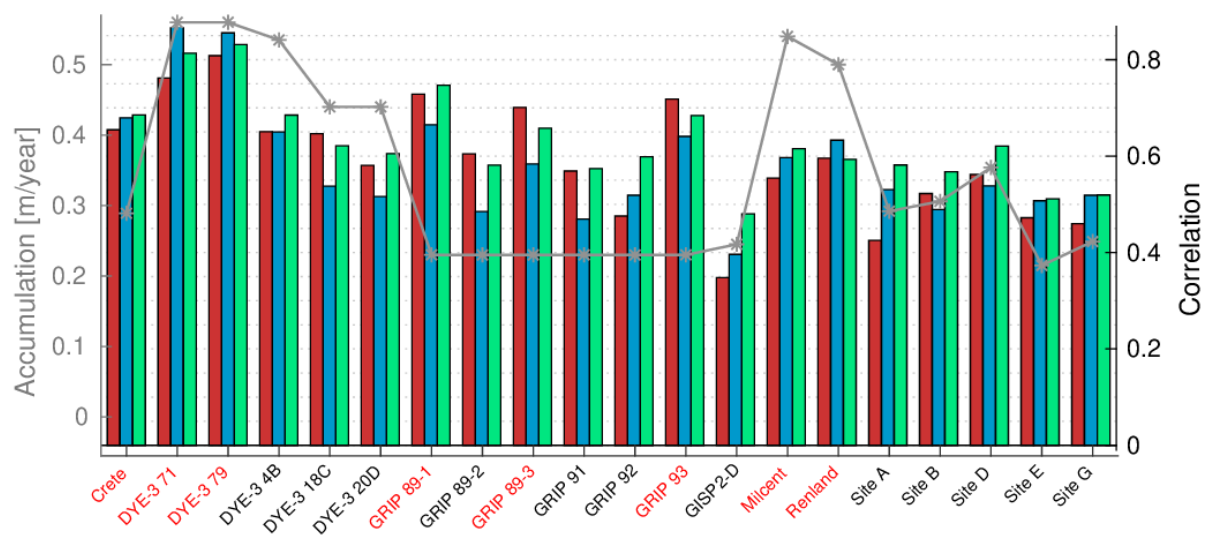


Figure S2: Accumulation at ice core sites (gray line, left axis) and correlation between reconstructed $\delta^{18}\text{O}$ and ice core $\delta^{18}\text{O}$ (Vinther et al., 2010) 1778-1970 for summer (red bars), winter (blue bars) and annual (green bars). This example is for reconstructions using 8 ice cores (names on axis in red) allowing the rest of the ice core data to be used as independent test data.

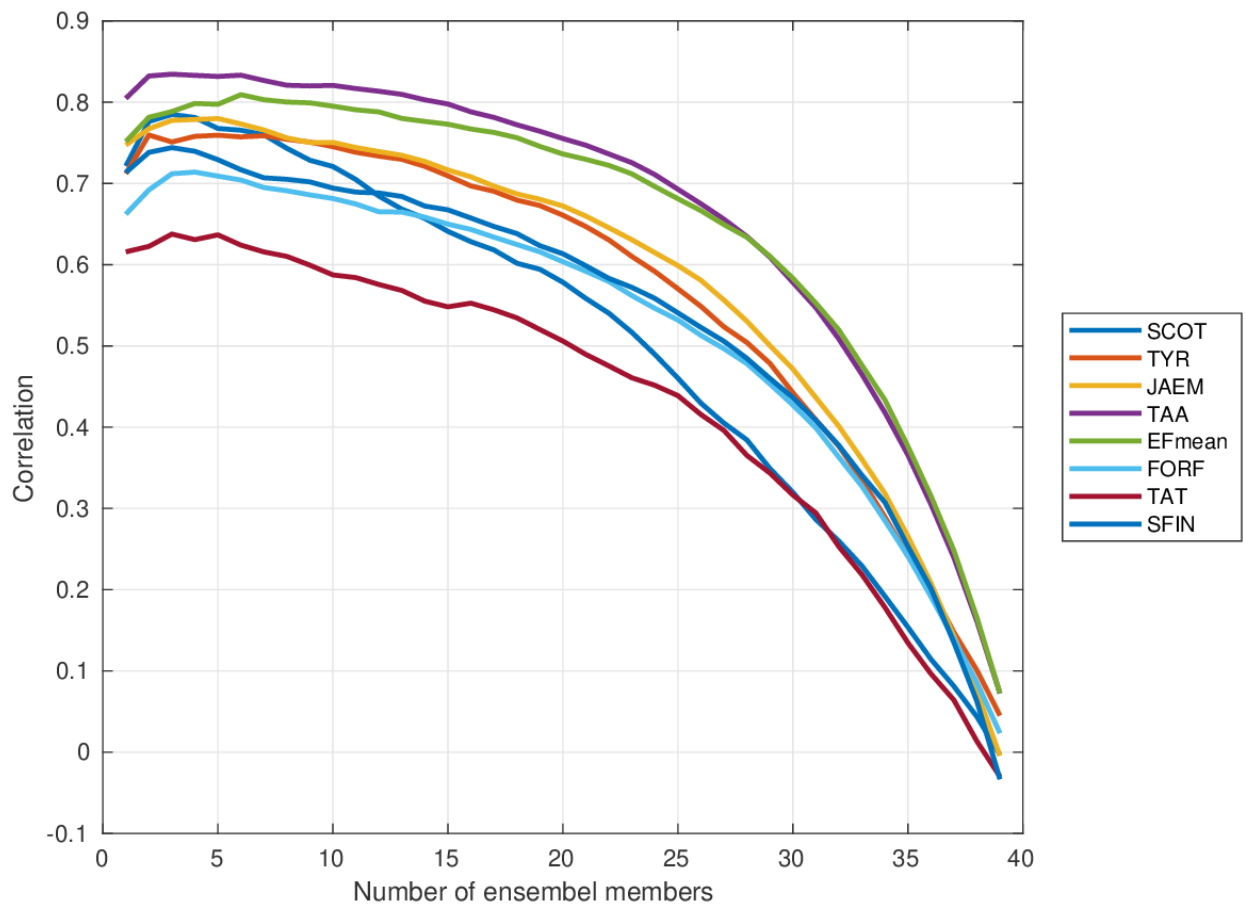


Figure S3: Correlation of reconstructed temperature for each tree ring site using increasing number of ensemble members.

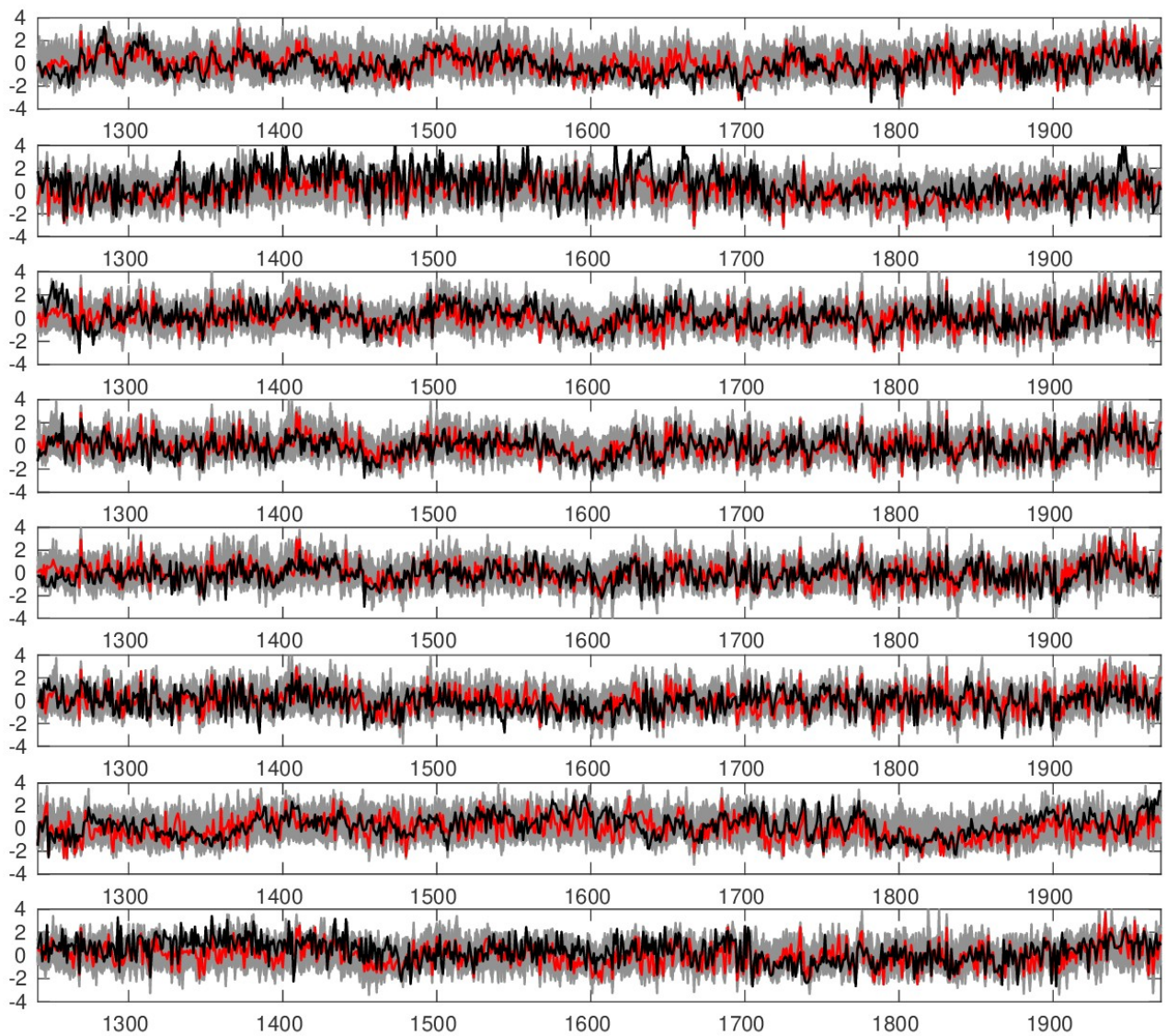
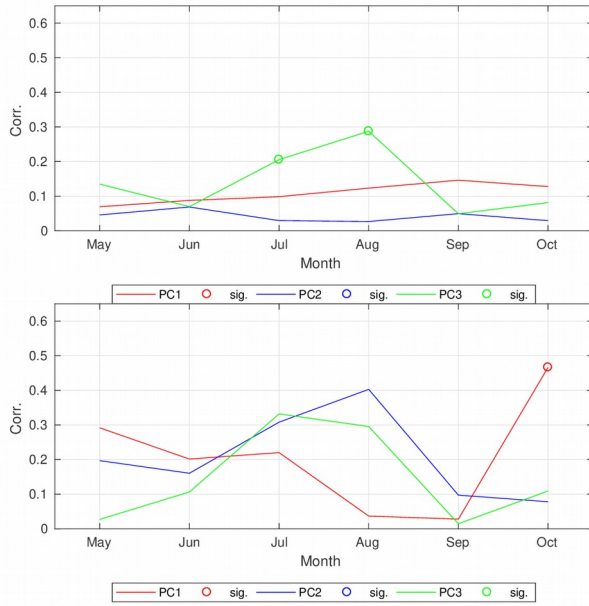
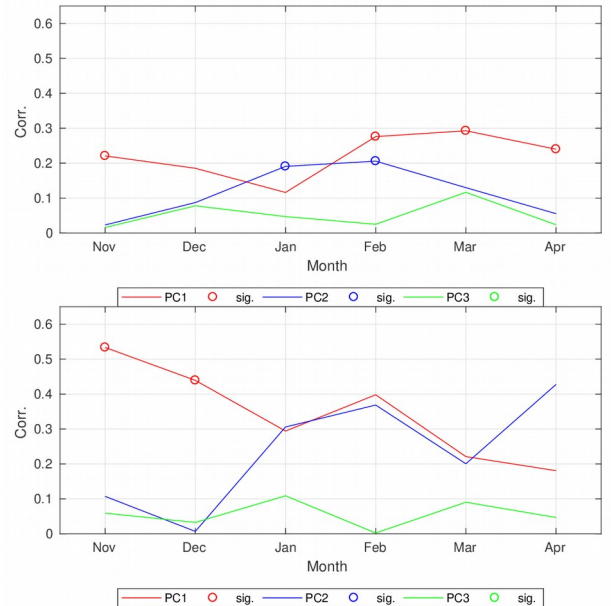


Figure S4: Comparison of reconstructed T2m at the tree ring sites with the tree ring data (black). The ensemble mean for 20 ensemble members is shown in red and all ensemble members are plotted in gray to show the spread. All data is normalized. The sites are (top to bottom): SCOT, TYR, JAEM, TAA, Efmean, FORF, TAT and SFIN.

Sum50, 8 ice cores



Win50, 8 ice cores



Win100, 8 ice cores

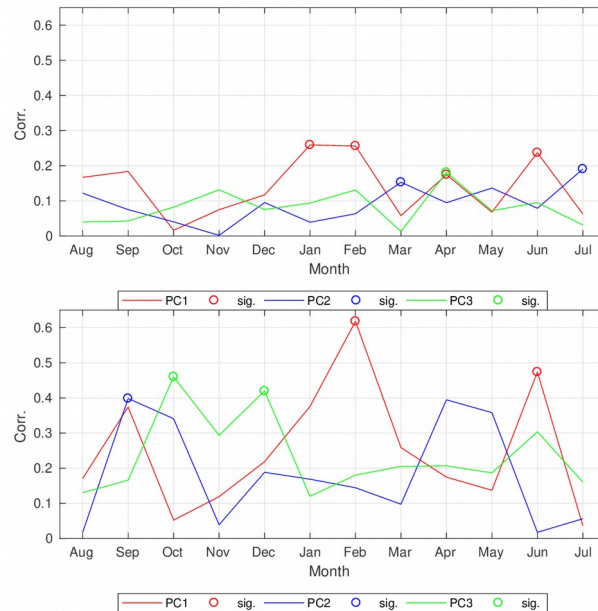
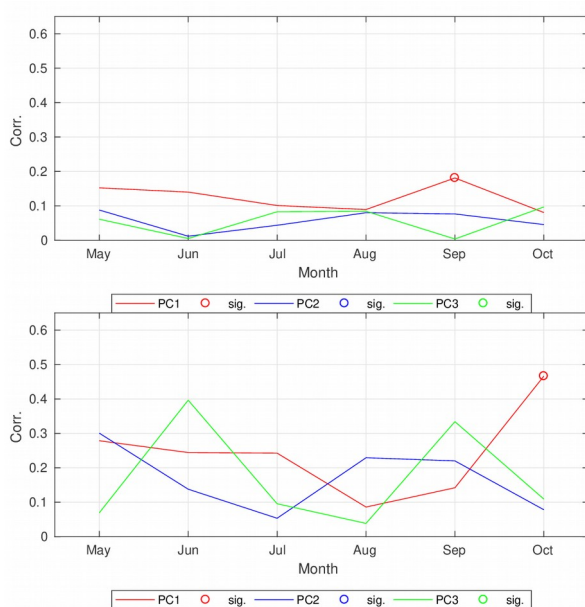
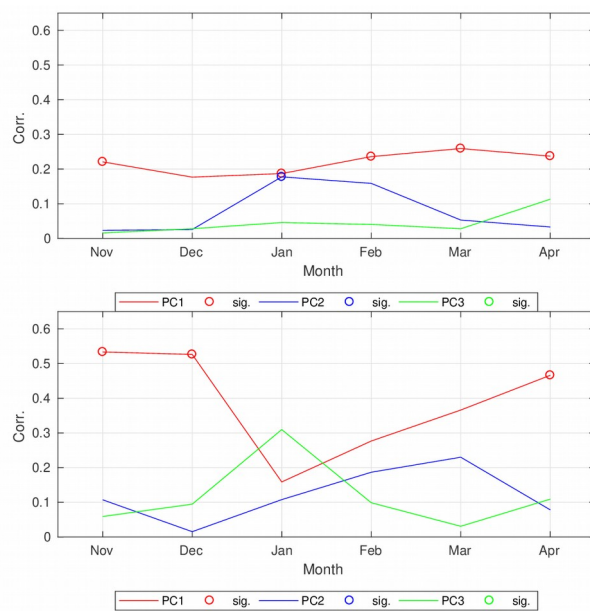


Figure S5: Test of monthly reconstructions based on 8 ice cores for sum50, win50 and win100. The first three PCs of reconstructed SLP are correlated against the PCs of 20CR SLP. The upper panel of each of the three subplots is for annual data, while the lower panel is for decadal filtered data. Circular markers indicate $p < 0.05$.

Sum50, 19 ice cores



Win50, 19 ice cores



Win100, 19 ice cores

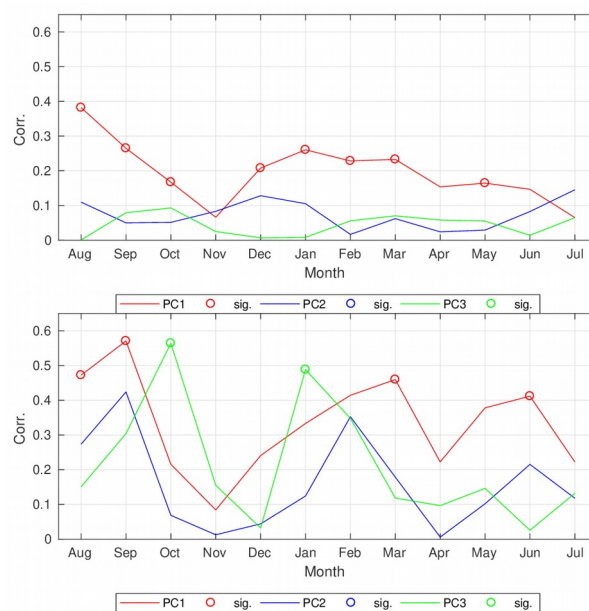


Figure S6: Test of monthly reconstructions based on 19 ice cores for sum50, win50 and win100. The first three PCs of reconstructed SLP are correlated against the PCs of 20CR SLP. The upper panel of each of the three subplots is for annual data, while the lower panel is for decadal data. Circular markers indicate $p < 0.05$.

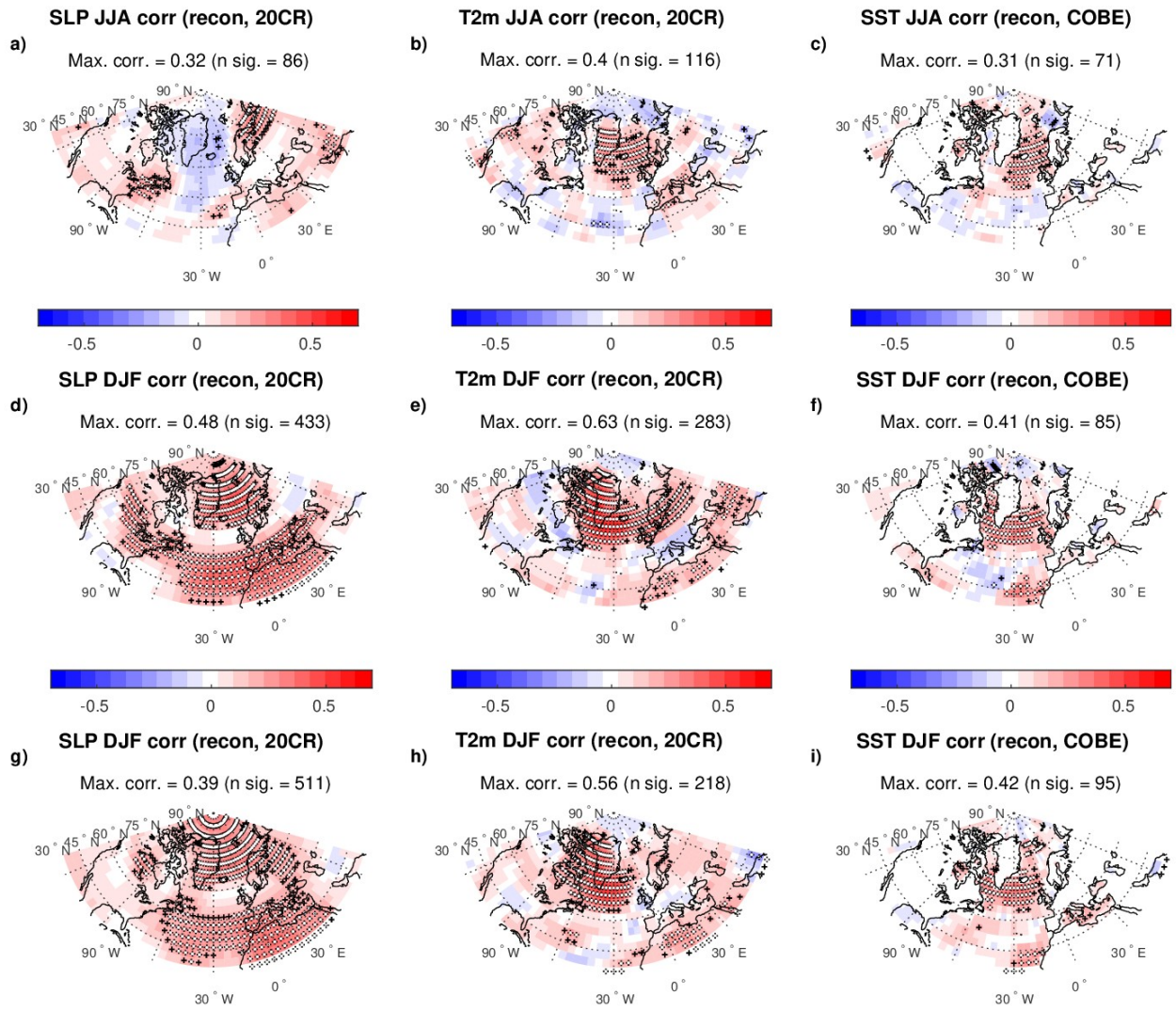


Figure S7: **(a-c)** Correlation between reconstructed (19 ice cores) and reanalysis SLP, T2m and COBE SST for JJA. The reanalysis data has been interpolated to the model grid (3.75 x 3.75 degrees). Black markers indicated $p < 0.05$ and white markers indicate $p < 0.025$. Also indicated is the maximum correlation (Max. Corr.) and the number of significantly correlated grid points (n sig.) ($p < 0.05$). **(d-f)** same as a-c, but for DJF. **(g-i)** same as a-c but for DJF reconstructed from the winter centered annual mean ice core data.

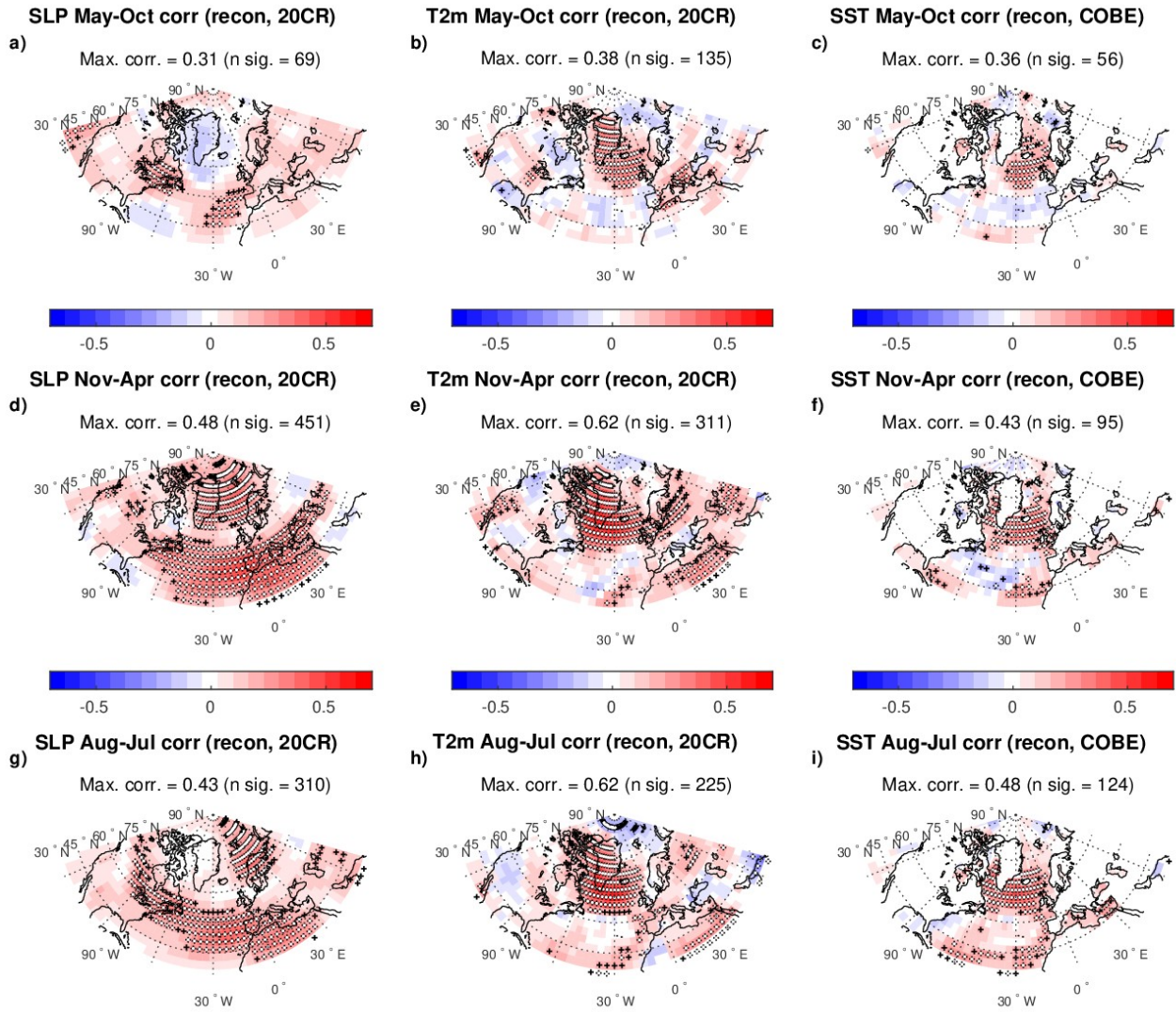


Figure S8: **(a-c)** Correlation between reconstructed (19 ice cores) and reanalysis SLP, T2m and COBE SST for sum50 (May-Oct). The reanalysis data has been interpolated to the model grid (3.75 x 3.75 degrees). Black markers indicated $p < 0.05$ and white markers indicate $p < 0.025$. Also indicated is the maximum correlation (Max. Corr.) and the number of significantly correlated grid points (n sig.) ($p < 0.05$). **(d-f)** same as a-c, but for Win50 (Nov-Apr). Bottom row: same as top row, but for the winter centered annual mean (Win100, Aug-Jul).

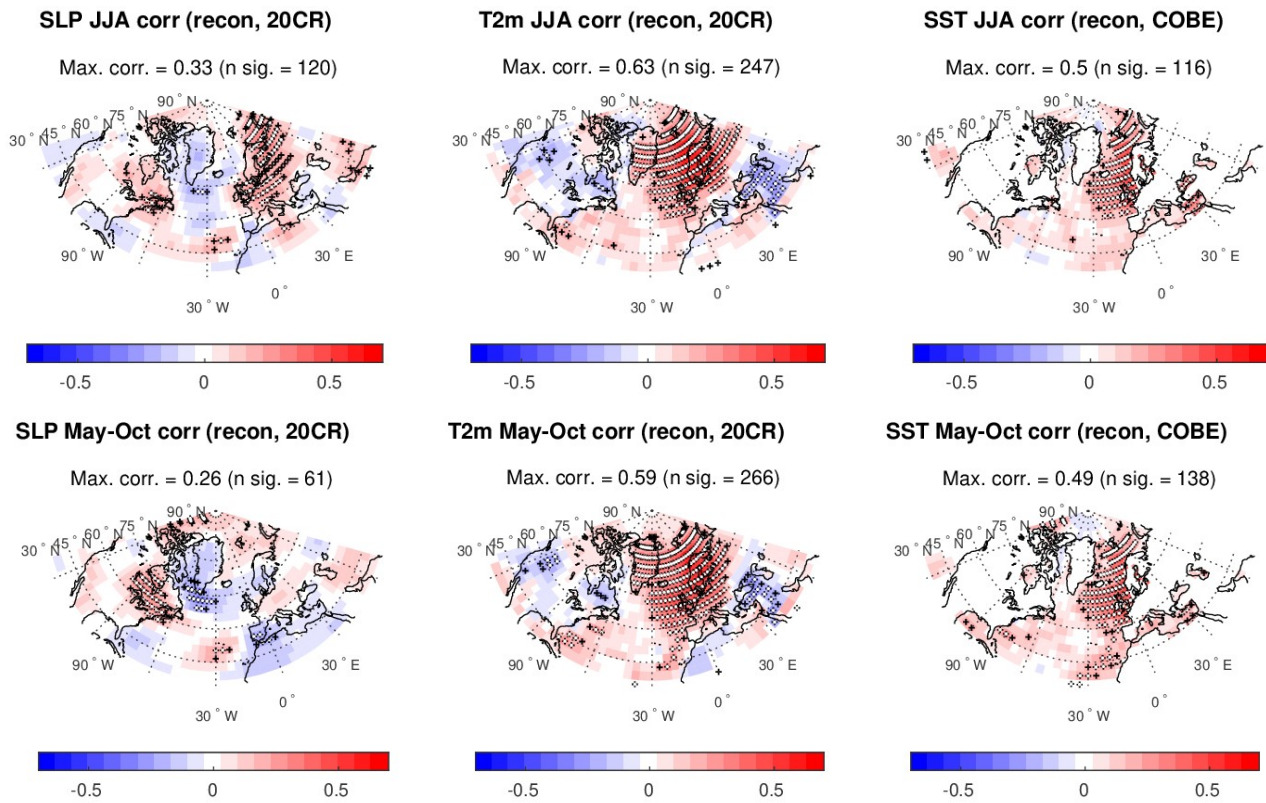


Figure S9: *Top row* Correlation between reconstructed and reanalysis SLP, T2m and COBE SST for JJA constrained by tree ring data. The reanalysis data has been interpolated to the model grid (3.75 x 3.75 degrees). Black markers indicated $p < 0.05$ and white markers indicate $p < 0.025$. Also indicated is the maximum correlation (Max. Corr.) and the number of significantly correlated grid points (n sig.) ($p < 0.05$). *Bottom row* same as top row, but for sum50 (May-Oct).

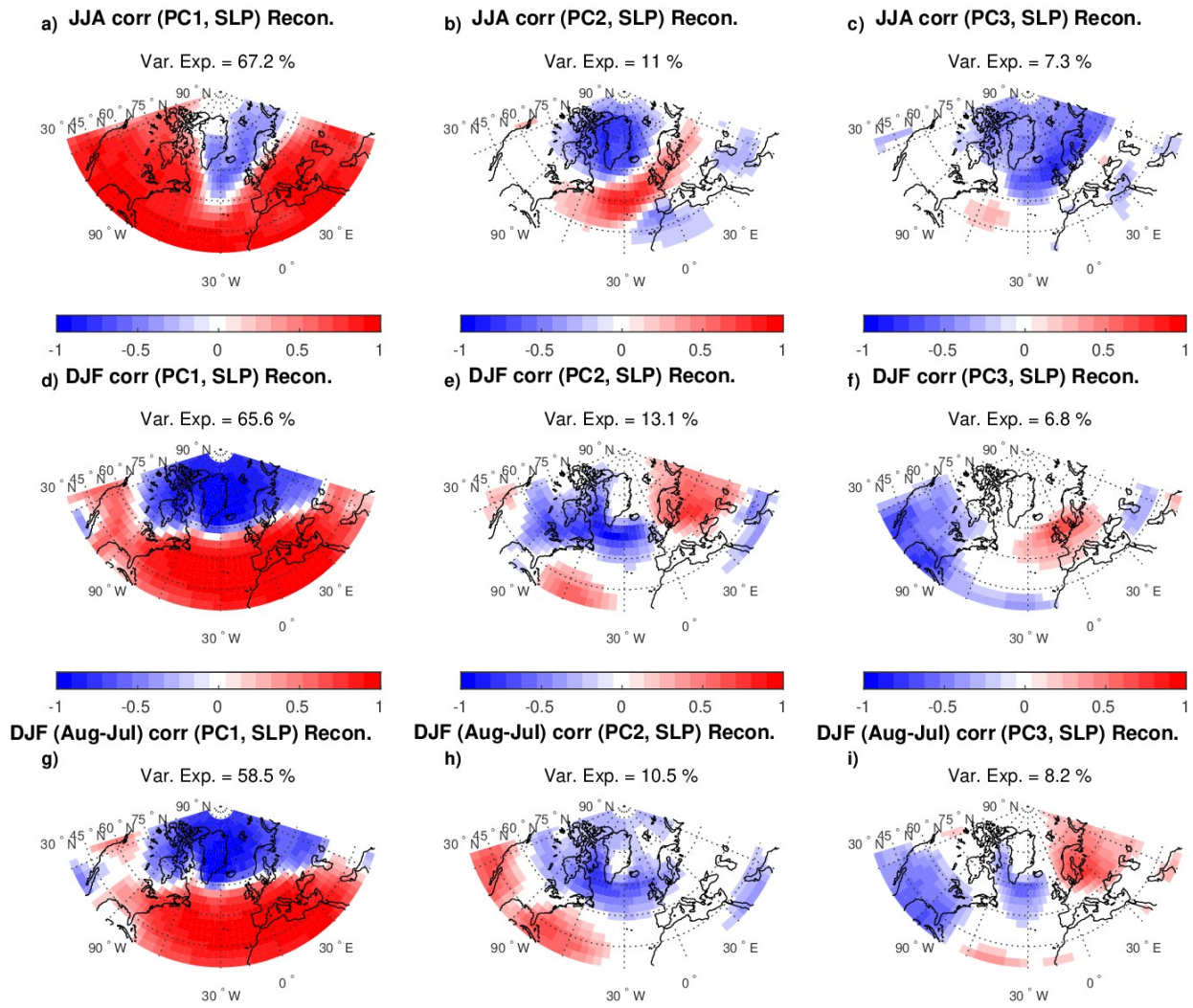


Figure S10: a)-c) regression of the first three reconstructed PCs of SLP on reconstructed (8 ice cores) JJA SLP, which corresponds to the reconstructed EOF patterns. d)-f) same as a)-c), but for DJF. g)-i) same as a)-c), but for DJF reconstructed (8 ice cores) from the winter centered annual mean ice core data. The time period is 1851-1970. Only data shown for $p < 0.05$.

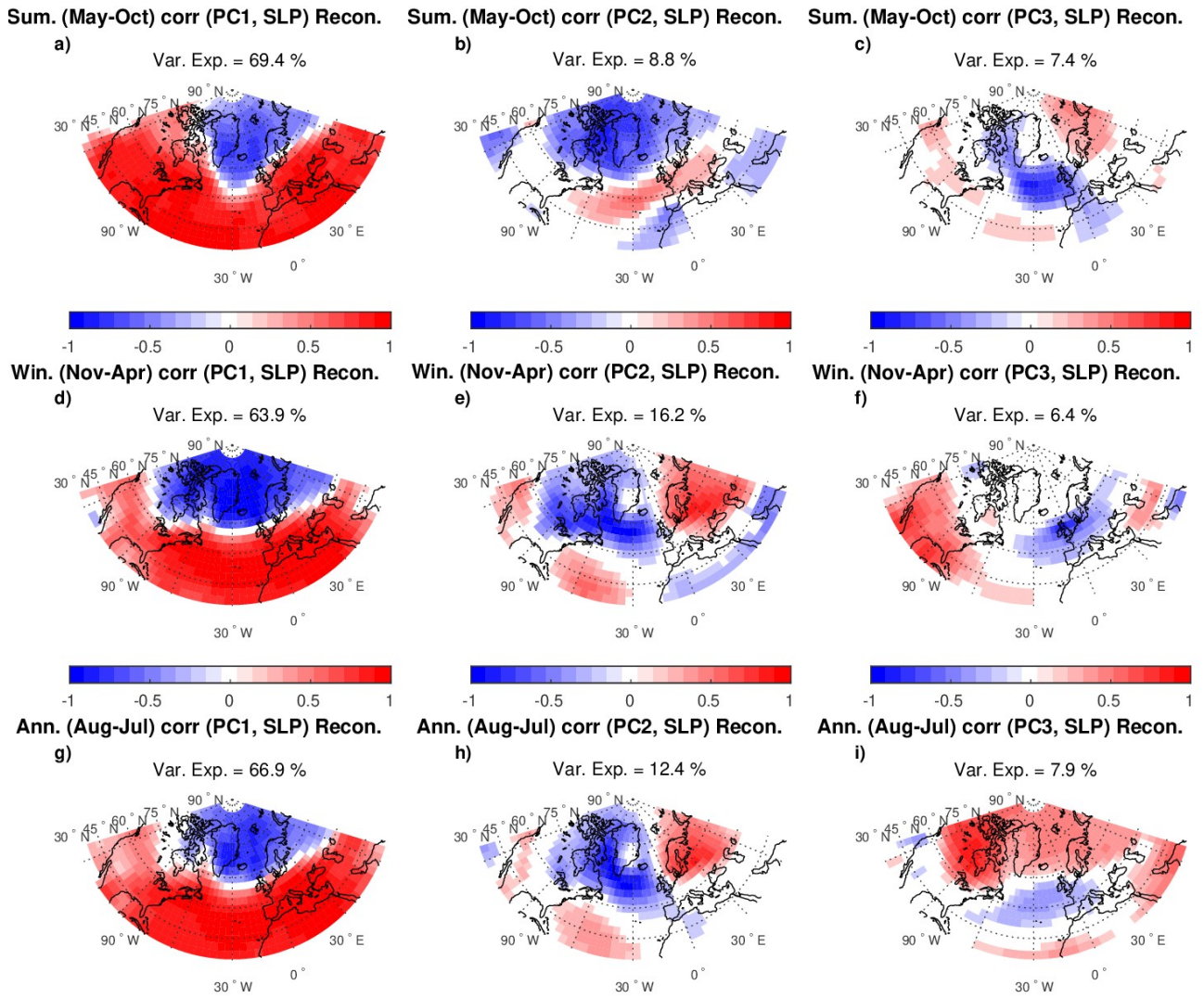


Figure S11: a)-c) regression of the first three reconstructed PCs of SLP on reconstructed (8 ice cores) Sum50 SLP, which corresponds to the reconstructed EOF patterns. d)-f) same as a)-c), but for Win50. g)-i) same as a)-c), but for the winter centered annual mean (Win100). The time period is 1851-1970. Only data shown for $p < 0.05$.

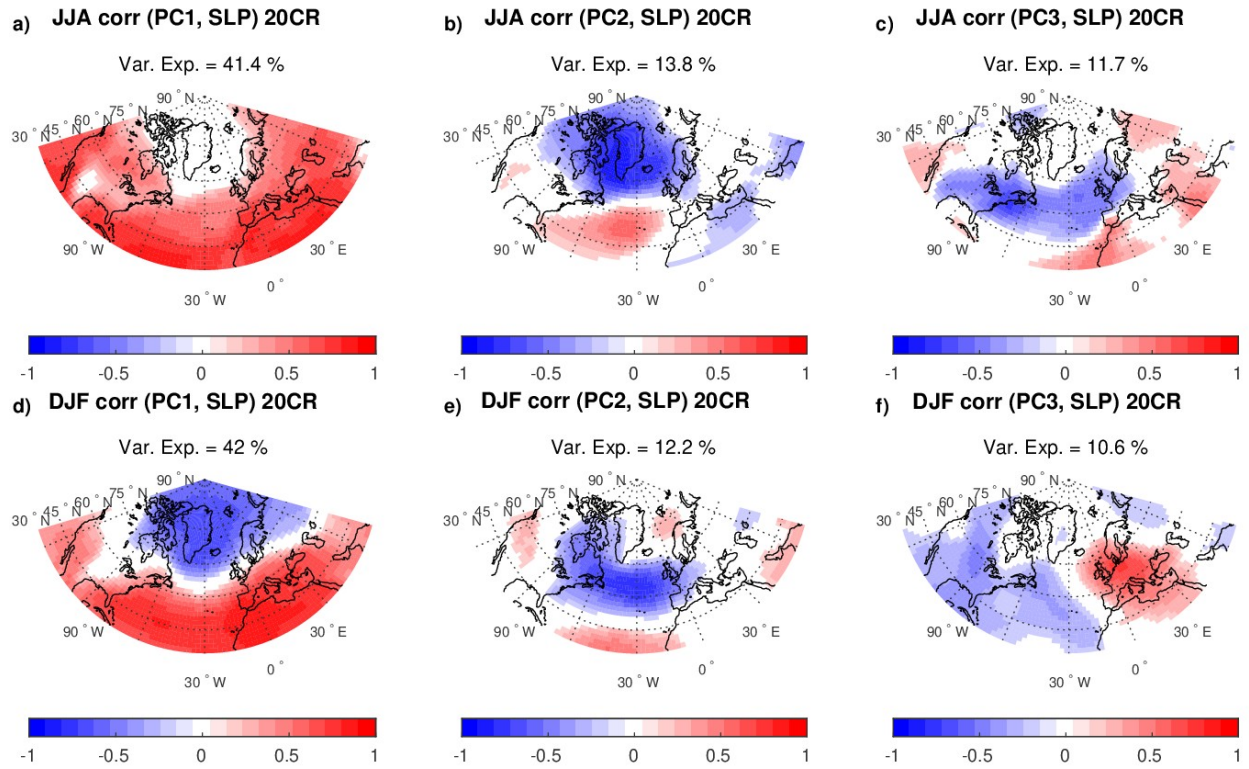
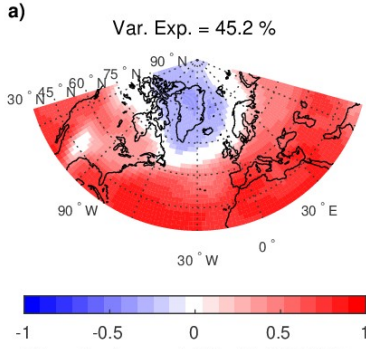
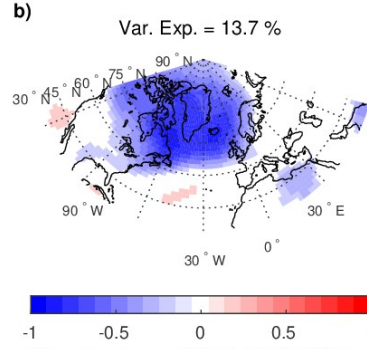


Figure S12: a)-c) regression of the first three 20CR PCs of SLP on 20CR JJA SLP, which corresponds to the EOF patterns. Top d)-f) same as a)-c), but for DJF. The time period is 1851-1970. Only data shown for $p < 0.05$.

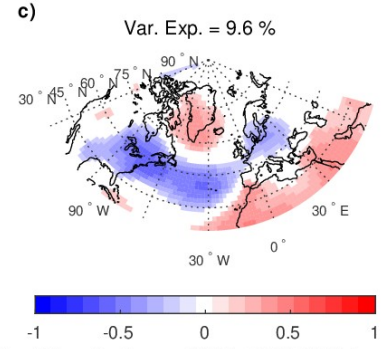
Sum. (May-Oct) corr (PC1, SLP) 20CR



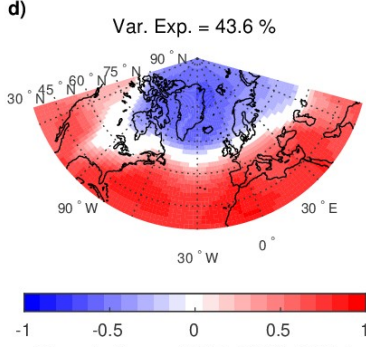
Sum. (May-Oct) corr (PC2, SLP) 20CR



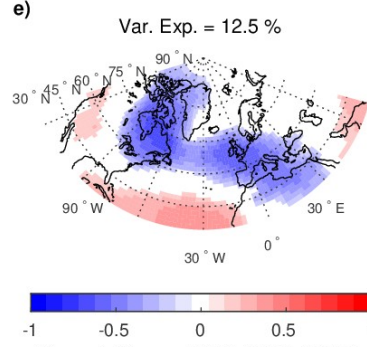
Sum. (May-Oct) corr (PC3, SLP) 20CR



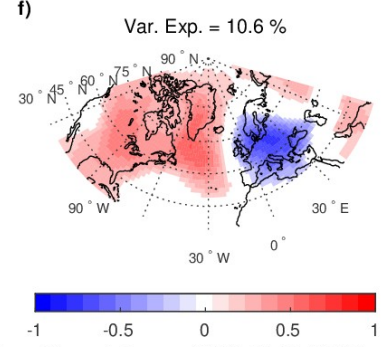
Win. (Nov-Apr) corr (PC1, SLP) 20CR



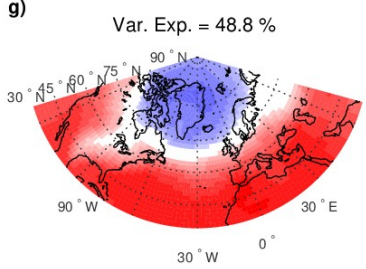
Win. (Nov-Apr) corr (PC2, SLP) 20CR



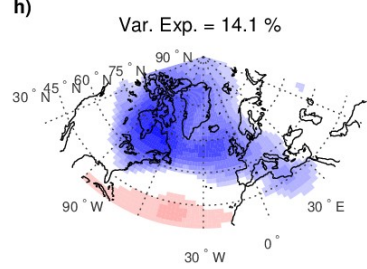
Win. (Nov-Apr) corr (PC3, SLP) 20CR



Ann. (Aug-Jul) corr (PC1, SLP) 20CR



Ann. (Aug-Jul) corr (PC2, SLP) 20CR



Ann. (Aug-Jul) corr (PC3, SLP) 20CR

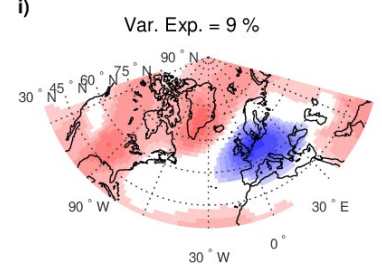


Figure S13: a)-c) regression of the first three 20CR PCs of SLP on 20CR sum50 (May-Oct) SLP, which corresponds to the reconstructed EOF patterns. d)-f) same as a)-c), but for Win50 (Nov-Apr). g)-i) same as a)-c), but for the winter centered annual mean (Win100, Aug-Jul). The time period is 1851-1970. Only data shown for $p < 0.05$.

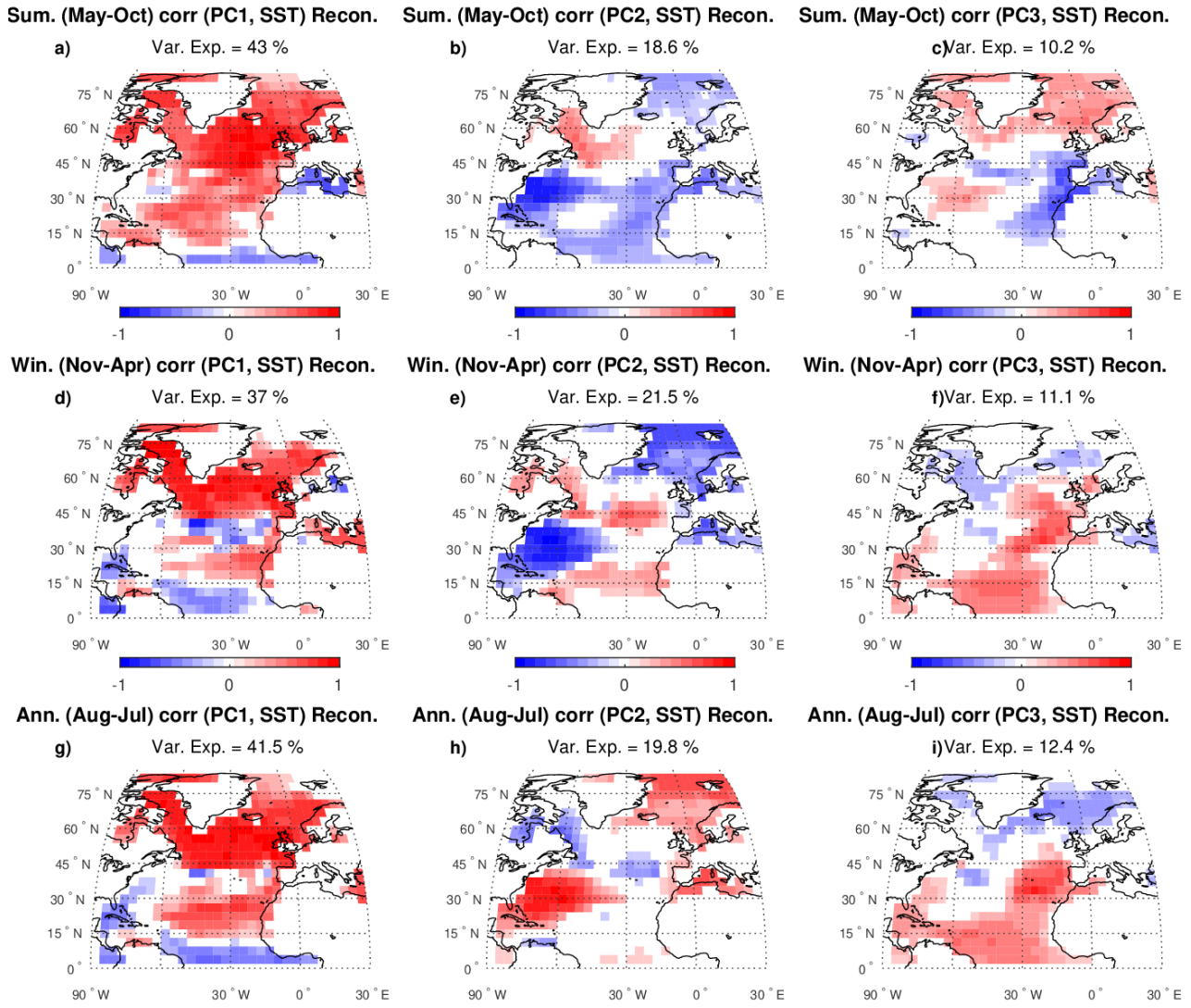
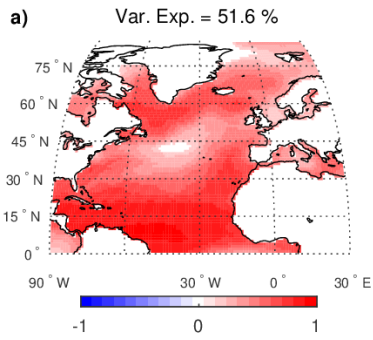
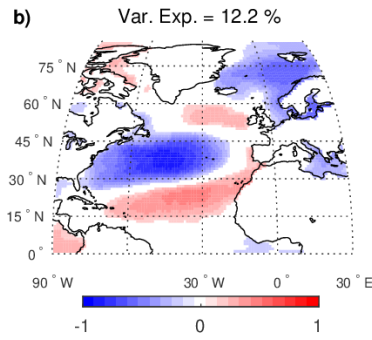


Figure S14: a)-c) regression of the first three reconstructed PCs of SSTs on reconstructed Sum50 SSTs, which corresponds to the reconstructed EOF patterns. d)-f) same as a)-c), but for Win50. g)-i) same as a)-c), but for the reconstructed winter centered annual mean (Win100, Aug-Jul). The time period is 1851-1970. Only data shown for $p < 0.05$.

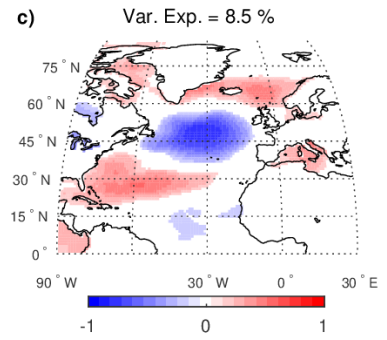
Sum. (May-Oct) corr (PC1, SST) 20CR



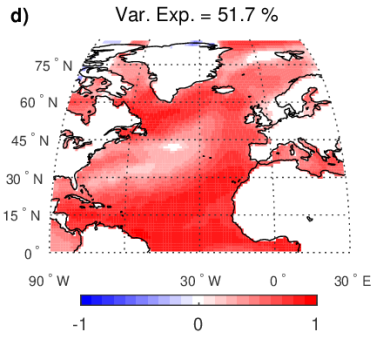
Sum. (May-Oct) corr (PC2, SST) 20CR



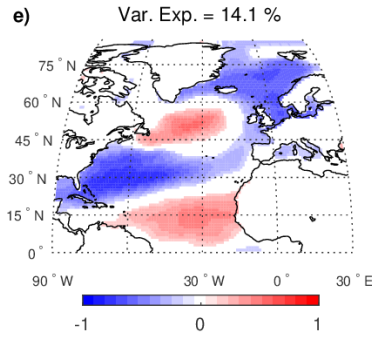
Sum. (May-Oct) corr (PC3, SST) 20CR



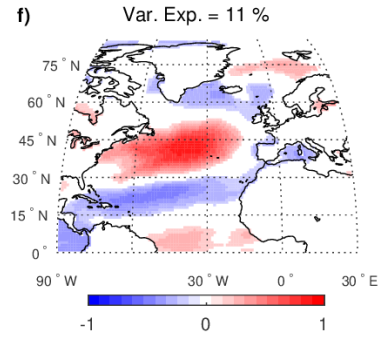
Win. (Nov-Apr) corr (PC1, SST) 20CR



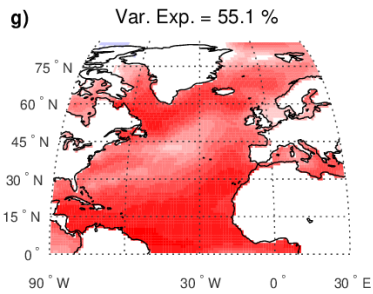
Win. (Nov-Apr) corr (PC2, SST) 20CR



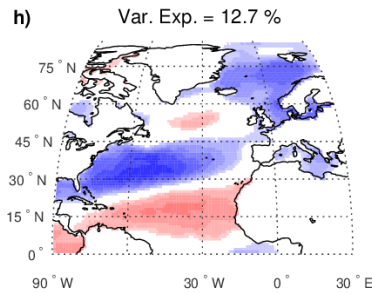
Win. (Nov-Apr) corr (PC3, SST) 20CR



Ann. (Aug-Jul) corr (PC1, SST) 20CR



Ann. (Aug-Jul) corr (PC2, SST) 20CR



Ann. (Aug-Jul) corr (PC3, SST) 20CR

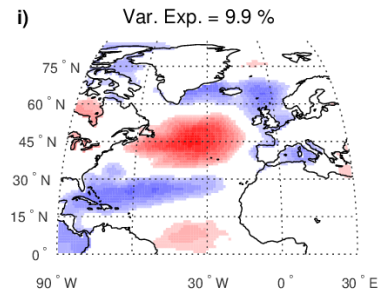


Figure S15: a)-c) regression of the first three COBE SST PCs on COBE sum50 (May-Oct) SSTs, which corresponds to the reconstructed EOF patterns. d)-f) same as a)-c), but for Win50 (Nov-Apr). g)-i) same as a)-c), but for the winter centered annual mean (Win100, Aug-Jul). The time period is 1851-1970. Only data shown for $p < 0.05$.

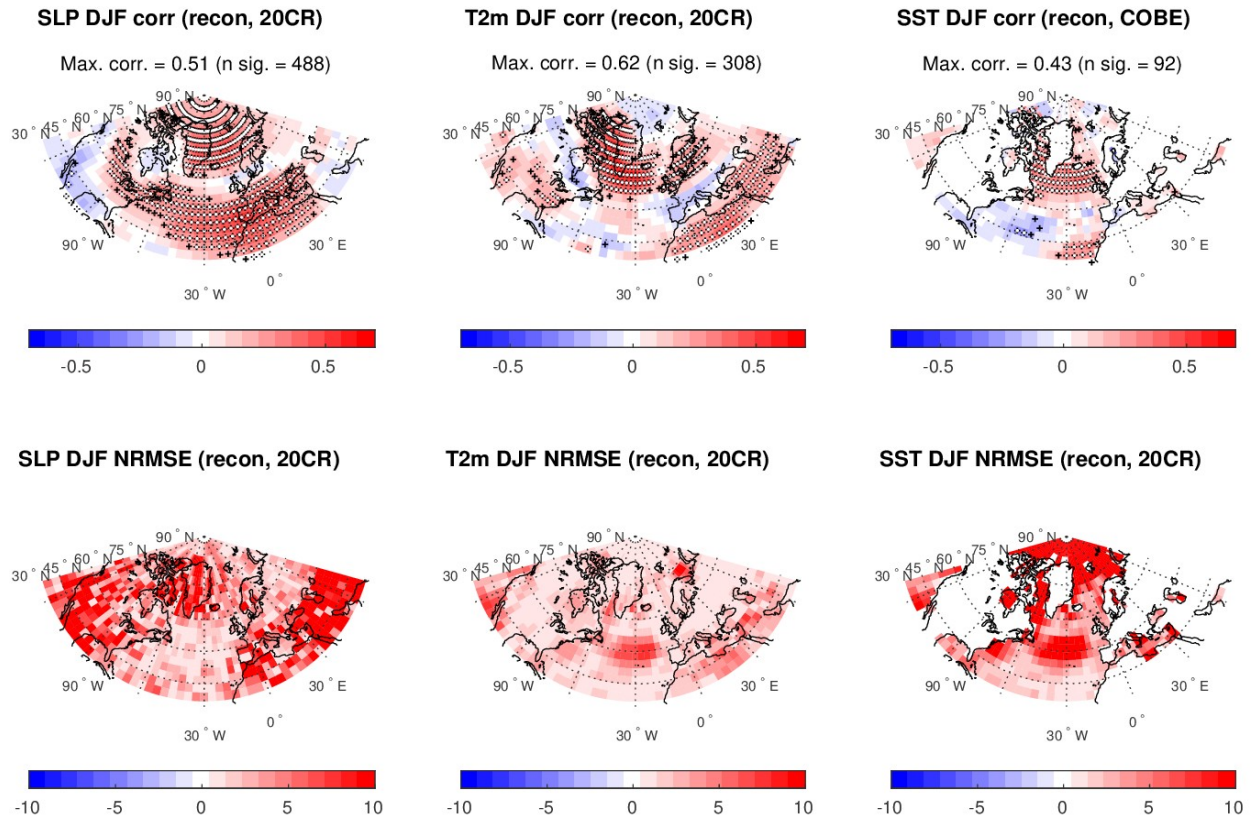


Figure S16: *Top row* Correlation between reconstructed (19 ice cores) and reanalysis SLP, T2m and COBE SST for DJF. The reanalysis data has been interpolated to the model grid (3.75 x 3.75 degrees). Black markers indicated $p < 0.05$ and white markers indicate $p < 0.025$. Also indicated is the maximum correlation (Max. Corr.) and the number of significantly correlated grid points (n sig.) ($p < 0.05$). *Bottom row* RMSE between reconstruction and reanalysis data normalized with the standard deviation of the reanalysis data (NRMSE). Generally the pattern of the NRMSE follows the skill in terms of correlation, such that areas of high correlation have low NRMSE. However, in coastal areas, and other areas of strong orography, as well as near sea ice the correlation can be significant, while the skill in terms of NRMSE can be poor.